



Study of the Effect of Laser Energy on the Structural and Optical Properties of TiO₂ NPs Prepared by PLAL Technique

Israa F. Hasan, Khawla S. Khashan*, Aseel A. Hadi

Department of Applied Sciences, University of Technology – Iraq

Article information

Article history:

Received: May, 16, 2021

Accepted: December, 19, 2021

Available online: March, 05, 2022

Keywords:

Laser ablation,
Physical properties,
Metal oxide nanoparticles,
TiO₂ NPs

*Corresponding Author:

Khawla S. Khashan
100082@uotechnology.edu.iq

Abstract

Titanium dioxide nanoparticles were produced in this work by laser ablation of a high purity titanium objective immersed in distilled water. Optical and structural properties of the obtained TiO₂ NPs using a Q-switched Nd: YAG laser of 1064nm wavelength with different laser energy (80, 100, 120, 140, and 160) mJ at 100 pulses was studied. The produced TiO₂ NPs were characterized employing UV-VIS Spectrophotometer, X-ray diffraction, and scanning electron microscopy (SEM). The obtained TiO₂NPs showed a decrease in transmittance in the region of the UV spectrum and an increase in the visible spectrum region. The estimated optical band gap of the TiO₂NPs was 3.89eV, 3.8eV, and 3.70eV at 80, 120 and 160mJ laser energy, respectively. The as-produced TiO₂NPs appear to be a Brookite crystalline phase with the preferential orientation along (200) direction. The scanning electron microscopy assays showed that the TiO₂ NPs have a cauliflower shape. Results show that with increasing the energy of laser pulse, the size of nanoparticles was increased noticeably. Where the particle size and its morphology are affected by laser energy.

DOI: [10.53293/jasn.2021.3600.1031](https://doi.org/10.53293/jasn.2021.3600.1031), Department of Applied Sciences, University of Technology

This is an open access article under the CC BY 4.0 License.

1. Introduction

Nanocrystalline TiO₂NPs are attracting great attention due to their broad variety of uses, such as photocatalysis, photoelectric conversion process in solar cells, antibacterial coatings, and gas sensors, thus titanium dioxide considers an important topic of research [1, 2]. Surface characteristics of NPs play a critical role in modifying bulk physical properties at the nanoscale, so many of the aforementioned applications are based on crystallographic structure, crystalline structure, and shape of nanoparticles [3, 4]. Because of its high internal activity, TiO₂ is among the first semiconductor photocatalysts to be examined and considers an active photocatalyst essential with the effect of ultraviolet radiation. Anatase (tetragonal), rutile (tetragonal), and Brookite (orthorhombic) are the three main distinctive primary crystalline phases of TiO₂ (bulk or nanoparticles). The rutile phase of TiO₂ is generally stable, whereas the anatase and brookite crystalline phases are semi-stable and quickly has converted to the rutile phase when is heated of over 600 to 800 degrees Celsius [5]. The Eg of anatase is approximately 3.2eV and 3.0eV for rutile. The third crystal phase, brookite, is the rarest naturally found phase of titania and is difficult to obtain in pure form. Brookite, like other phases, is photo-catalytically active [6]. There are many different methods to produce TiO₂ nanoparticles, such as sol-gel, chemical vapour deposition (CVD), spray pyrolysis, mechanical method (Milling), and laser ablation. Laser ablation is a unique technique of basic interest to

fabricating TiO₂ nanoparticles in the liquid phase, and also a promising technique for handling nonmaterial production by quick reactive quenching of ablated species at the interface of plasma-liquid.

The PLAL method for preparing nanoparticles from a solid target in a liquid medium has a number of advantages. Firstly, is the low cost of ablation environment-keeping devices. Secondly, it does not use chemical substances. Thirdly, it creates free-contamination nanoparticles without polluting the environment [7]. Many researchers have focused on the preparation of TiO₂ nanoparticles, for instance; A. Singh, et al. [8] have used pulsed laser ablation to prepare TiO₂ nanoparticles in water and reported the influence of laser power on generated TiO₂NPs. They found that the generated TiO₂ NPs showed an increase in the yield NPs with increasing laser power. Also, V.A. Zuñiga-Ibarra, et al. [9] used pulsed Nd: YAG laser with a 532 nm wavelength in their study, black TiO₂ nanoparticles were created by irradiating white TiO₂ nanoparticles in water. Recently, Amir R. Sadrolhossini et al. [10] have used laser ablation techniques to create titanium oxide nanoparticles in an aqueous solution containing carbon quantitative points. The prepared sample was utilized to detect sugar and the sample's sensitivity. Where glucose was detected more readily than other sugars. The detection limit was 0.01 parts per million. More, recently N. Pashazadeh Kan et al. [11] have prepared TiO₂ nanoparticles in water using the PLAL method and investigated the effect of SDS incorporation.

In the PLAL technique, a laser (in pulsed operating mode) irradiates a highly pure target immersed in a liquid to synthesis particles of different sizes. Cavitation bubbles form due to the water optical breakdown via the pulsed laser, which the generation and growth of NPs carry out inside. Upon the breakdown of the cavitation bubble, such nanoparticles released into the surrounding solvent forming a suspension of NPs [12]. Due to the abundance of numerous lasers, no definite outcomes on the influence of the parameters of the laser, such as laser density and laser energy, on the product of the synthesis of TiO₂ nanoparticles. The aim of this research is to satisfy this study gap by experimental examination of disparity in the synthesis yield of nanoparticles. In the current research, we determined how the laser energy affects the physical properties of the prepared TiO₂ nanoparticles.

2. Experimental Procedure

Colloidal NPs Synthesis:

A 99.99% pure titanium (Ti) target was used to synthesis TiO₂NPs in deionized water by a nanosecond pulsed laser. A Ti plate was placed in the bottom of a glass vessel (see Figure 1) the distilled water level over the target is approximately 3ml. A pulsed Q-switched Nd: YAG laser parameters are shown in Table 1. The laser ablation process in deionized water was continuous for 10 minutes. Since water absorbs significantly at a wavelength of 1064 nm, the impact of the water level of the laser beam intensity and focal length were considered and recalculated. During laser irradiation of the Ti objective, the plume of plasma is clearly visible with a naked eye. This is due to the ablation process.

Table 1: Laser beam parameters used in preparation of TiO₂ nanoparticles

	Parameters	Value
Laser beam	Wavelength (λ)	1064 nm
	Repetition rate	1 Hz
	pulse duration	9 ns
	Beam diameter	2.4 mm
	built-in lens focal length	120 mm
	Laser pulse energy	(80, 100, 120, 140, and 160) mJ
	No. of pulses	100 pulse
	Ablation time	10 minutes
Materials	Target	Titanium metal
	Liquid	De-ionized water

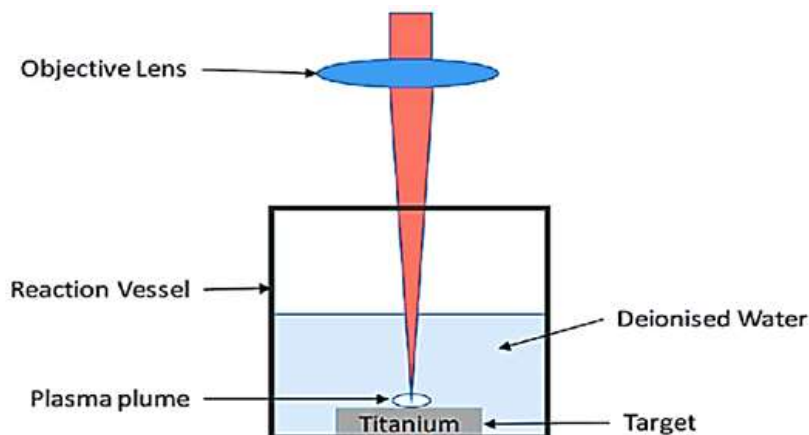


Figure 1: A schematic representation of ablation process of titanium target in water by laser [10].

3. Characterization of TiO₂ NPs

3.1. Nanoparticles Concentration in Deionized Water

To estimate the amount of content ablated, a 4-digit sensitive scale was utilized. It was calculated by weighing the objective firstly before the ablation process and secondly after the completion. This process is repeated each laser energy. Following the ablation procedure, the target was dried before being weighed. The quantity of the ablated mass (ΔM) is:

$$\Delta M (mg) = mb - ma \dots \dots \dots (1)$$

Where mb is target mass before ablation process and ma is target mass after ablation process.

The mass concentration was found by:

$$\text{Mass concentration} = \Delta M / \text{liquid criterion} (mg / ml) \dots \dots \dots (2)$$

3.2. UV-Visible Spectroscopy

The UV-visible absorption spectra of as-prepared titanium oxide colloid by laser in water within the spectral range (200-1100nm) were registered and examined using a dual-beam UV-VIS spectrophotometer (model SP-3000 Plus, OPTIMA). The optical properties of the NPs solution were tested by using an optical cell (quartz) with an optical path of 1cm.

3.3. X-ray Diffraction (XRD)

X-Ray diffraction (XRD) measurements of the metal oxide nanoparticles solution were performed using a (Philips PW) Cu-K radiation source at 2 angles= (20-80) degree. X-Ray diffraction is a method for determining a material's phase. The sample for X-ray assay was prepared by dropping of solution on a glass substrate and then dried in the air environment. The Scherer formula was used to measure the grain size from the distance of the XRD peaks. [13].

$$D = 0.94 \lambda / \beta \text{Cos } \theta \dots \dots \dots (3)$$

Where λ is the X-ray wavelength (1.54060 Å), β the full-width at half maximum of diffraction line in radian, and θ is diffraction angle.

4. Results and Discussion

4.1. Mass Concentrations

Figure 2 describes the laser energy effect on the mass concentration of TiO₂NPs in distilled water (calculated using equations (1 & 2)), where laser energy was altered from 80 to 160 mJ for 10 minutes of ablation. The concentration

of NPs in the suspension, increased gradually with increasing laser energy, as shown in figure2. This is may be attributed to the increase evaporation of the target due to the increase surface temperature results from an increase in laser energy.

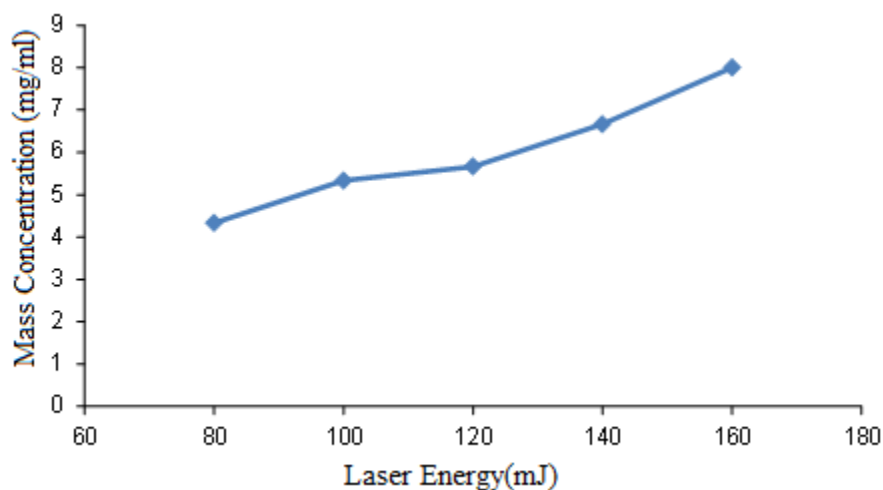


Figure 2: Mass concentration of ablated TiO₂ NPs versus laser energy.

The amount of generated NP is affected by factors correlated with the target's optical and thermal properties, such as light absorption on the target surface, reflectivity, heat energy, vapor enthalpy, boiling point, and thermal conductivity [14].

4.2. UV-Visible Spectroscopy

Figure 3 shows the UV-Vis transmittance spectra of the TiO₂ colloidal prepared using a 1064nm laser with various laser energy (80,100,120,140, and 160) mJ at 100 pulses for a continuous ablation period of 10 minutes. UV-VIS measurements were performed at wavelengths ranging from 200 to 1100 nm. From these results, we noticed that by increasing laser energy of the ablation, the transmittance decreased in the region of the UV spectrum and increased in the region of the visible spectrum, where the light transmittance exceeded 99% in regions of the visible spectrum. Still, the samples are transparent to the visible light. This indicates that the generated TiO₂ NPs can be used as a photocatalytic material [15].

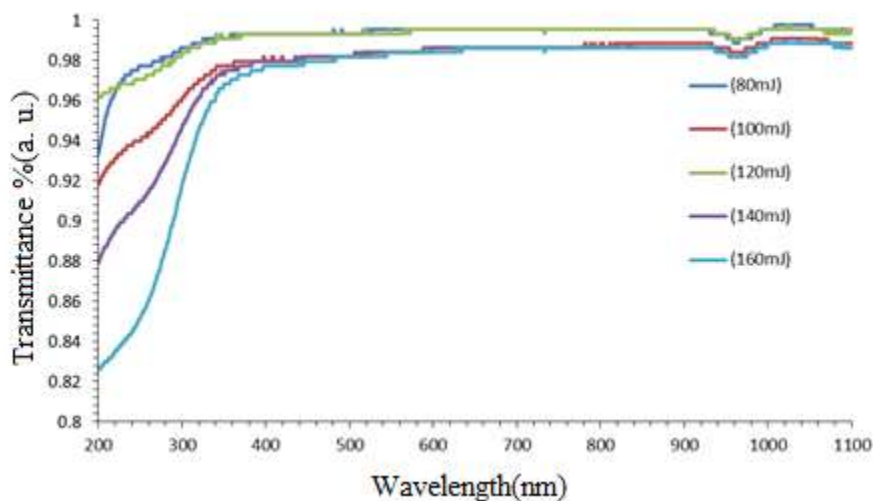


Figure 3: Transmittance spectra of the TiO₂ NPs colloidal synthesised with different laser energy at 100 pulses.

Tauc's relation was used to measure the optical band gap of the produced NPs as follows [16]:

$$(\alpha h\nu)^n = K(h\nu - E_g) \dots \dots \dots (4)$$

Where α is the absorption coefficient, $h\nu$ is photon energy, E_g is the optical band gap of NPs, K is a constant of effective mass which associates with the valance and conduction bands, n is number that determines the type of electronic transition that leads to the absorption and takes values 2 or $\frac{1}{2}$ depending whether the transition is direct or indirect respectively. The linear line obtains by drawing $(\alpha h\nu)^2$ against $h\nu$ which refers to the band gap of colloids NPs after its intersection with $h\nu$ -axis which shows the direct transition. The band gap values of TiO_2 NPs were (3.89, 3.8 and 3.70) eV; are corresponding to the TiO_2 NPs prepared with (80,120, and 160) mJ, respectively, and are greater than the TiO_2 bulk due to the particle size reduction caused by quantum confinement and an upsurge of surface/volume ratio [17, 18].

Figure 4 shows that as the laser energy increases, the optical band gap gets narrows. This decrease in energy gap value could be attributed to barred impurities, which resulted in donor levels of energy gaps near the conduction band get close to that at lower energies. A few TiO_2 nanoparticles are ablated from the target, and the monitored band gap energies at 80mJ, 120mJ, and 160mJ are 3.89eV, 3.8eV, and 3.70eV, respectively. As the laser energy increases, so does the number of nanoparticles on the target's surface, causing the shielding effect to appear near the target's surface and fragmenting the nanoparticles created in previous stages [7].

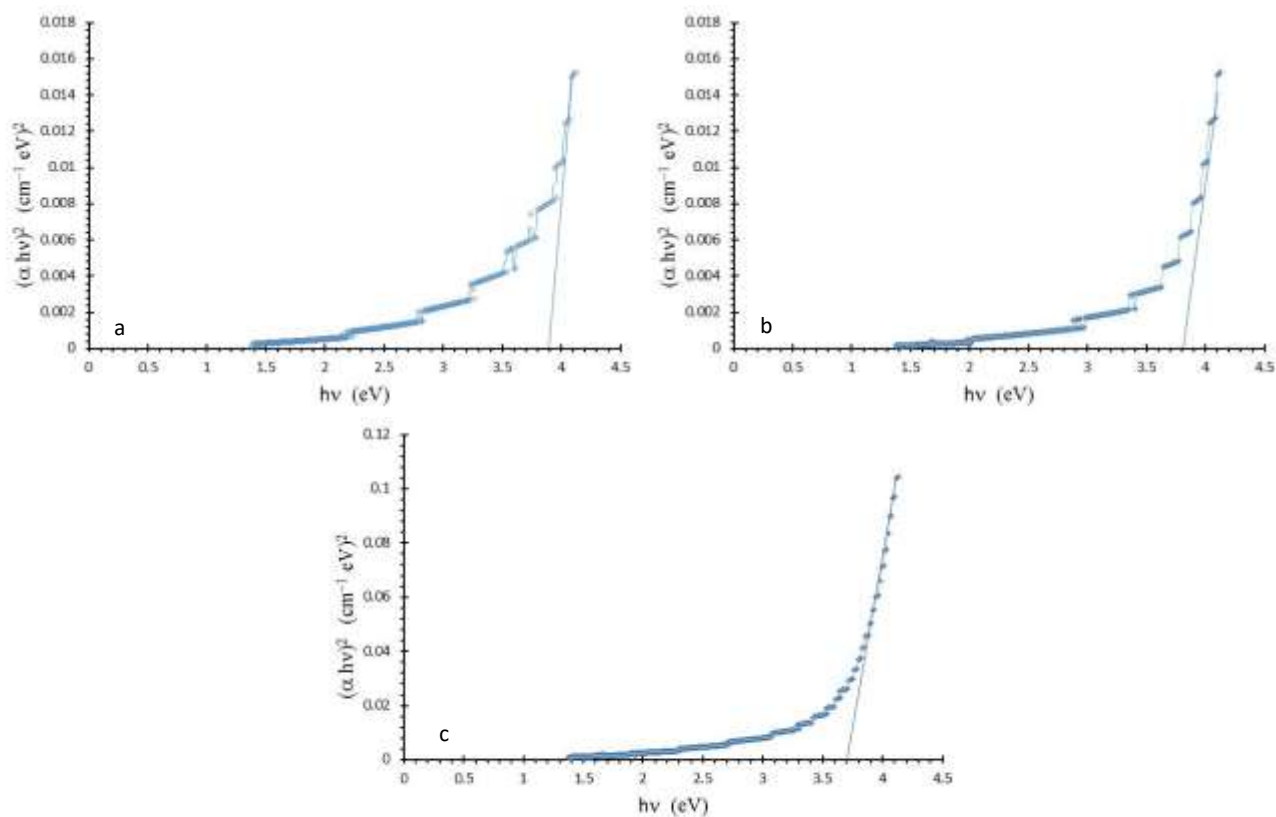


Figure 4: The optical band gap of TiO_2 NPs prepared at different laser energy (a) 80mJ (b) 120mJ, and (c) 160mJ.

4.3. X-ray Diffraction (XRD)

To investigate the XRD pattern of TiO_2 nanoparticles, several numbers of suspensions of nanoparticles were obtained via pulsed laser ablation with various laser energies and then were deposited onto the glass substrate separately. Figure 5 shows the XRD patterns of prepared NPs. As it is obvious, a different diffraction peaks exist for nanoparticles prepared with different laser energies, and the intensity of these peaks differs between samples. The X-ray diffraction patterns of specimens show a main peak at $2\theta=33^\circ$, which is attributed to the diffraction of

X-ray photons from the crystal lattice for TiO₂'s Brookite phase assign to the plane of (200) [5, 19]. For all the prepared samples, Brookite phase with a small fraction of Anatase phase of a (201), (121), (200) and (400) reflection plane of some peaks were observed. The absence of the rest of the peaks compared to the standard XRD diffraction pattern can be attributed to the low concentration of the prepared nanoparticles colloidal, and it may be due to its deposition on an amorphous glass substrate. The Scherrer equation (Eq. (5)) was used to calculate the average particle diameter (d) of TiO₂ nanoparticles in the most intense peak (200) plane.

$$d = (0.9\lambda/\beta \cos\theta) \dots \dots \dots (5)$$

Where: d is the average crystalline size, 0.90 is the Scherrer constant, λ is the X-Ray wavelength of 1.54056 Å, β is full width half at maximum and θ is the Bragg's diffraction angle. Whereas, particle size diameter of TiO₂ nanoparticles has been calculated to be 23.1 nm.

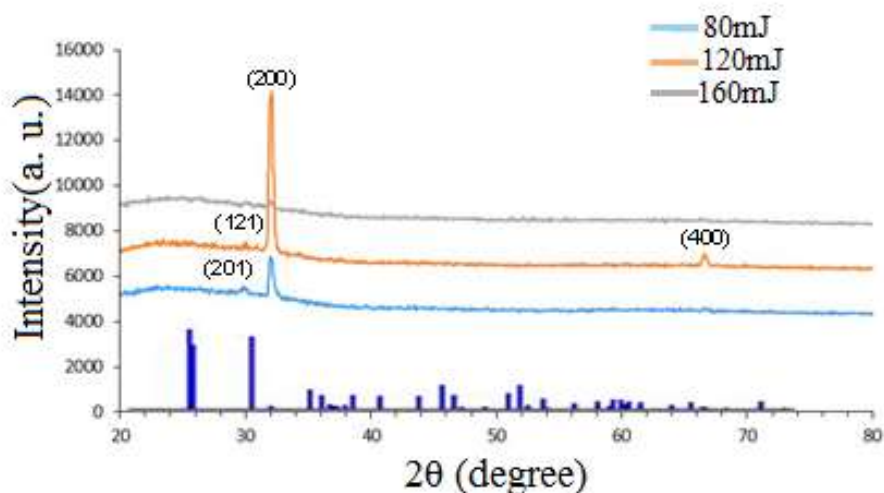


Figure 5: XRD spectra of the TiO₂NPs prepared at different laser energy standard XRD peaks positions pattern of Brookite TiO₂ placed on x-axis

4.4. Scanning Electron Microscope (SEM) Investigations

Figure 6 shows SEM micrographs of TiO₂NPs synthesized by pulsed laser ablation of the Ti target at a) 8mJ, b) 120mJ, and c) 160mJ laser energy in DIW. According to the images, the formed nanoparticles are found to be uniformly distributed and have a cauliflower-like shape with a new and distinctive shape that differs from the rest of the nanoparticle shapes resulting from the PLAL technique in previous researches; in which most of particles are connected to form a cluster of nanoparticles (Figure 6a-c). All samples were symmetric in shape with an increase in size of nanoparticles with the increase of laser energy. The increase in laser energy leads to the temperature and pressure of the plasma plume be higher. Thus, a longer period of the cavitation bubbles results in the enhancement of the formation of bigger particle via coalescence [13]. This is consistent with UV-VIS results. The primary pulses of laser can allow to generating of some nanoparticles; such NPs may suspend in the path of the subsequent incident laser pulse [20]. These formed nanoparticles can absorb the photon energy of the next strikes of laser pulses, and this effect enhances with the increase of laser energy due to the increases in the number of synthesized nanoparticles. This leads to a decrease in the intensity of the laser beam that can reach the objective as a result of the laser light absorption by such nanoparticles. The Increase of the laser energy increases the synthesize rate of the TiO₂ nanoparticles [21]. Thereby, the local concentration of ablated species increases sharply with such parameters due to the liquid confinement [22, 23].

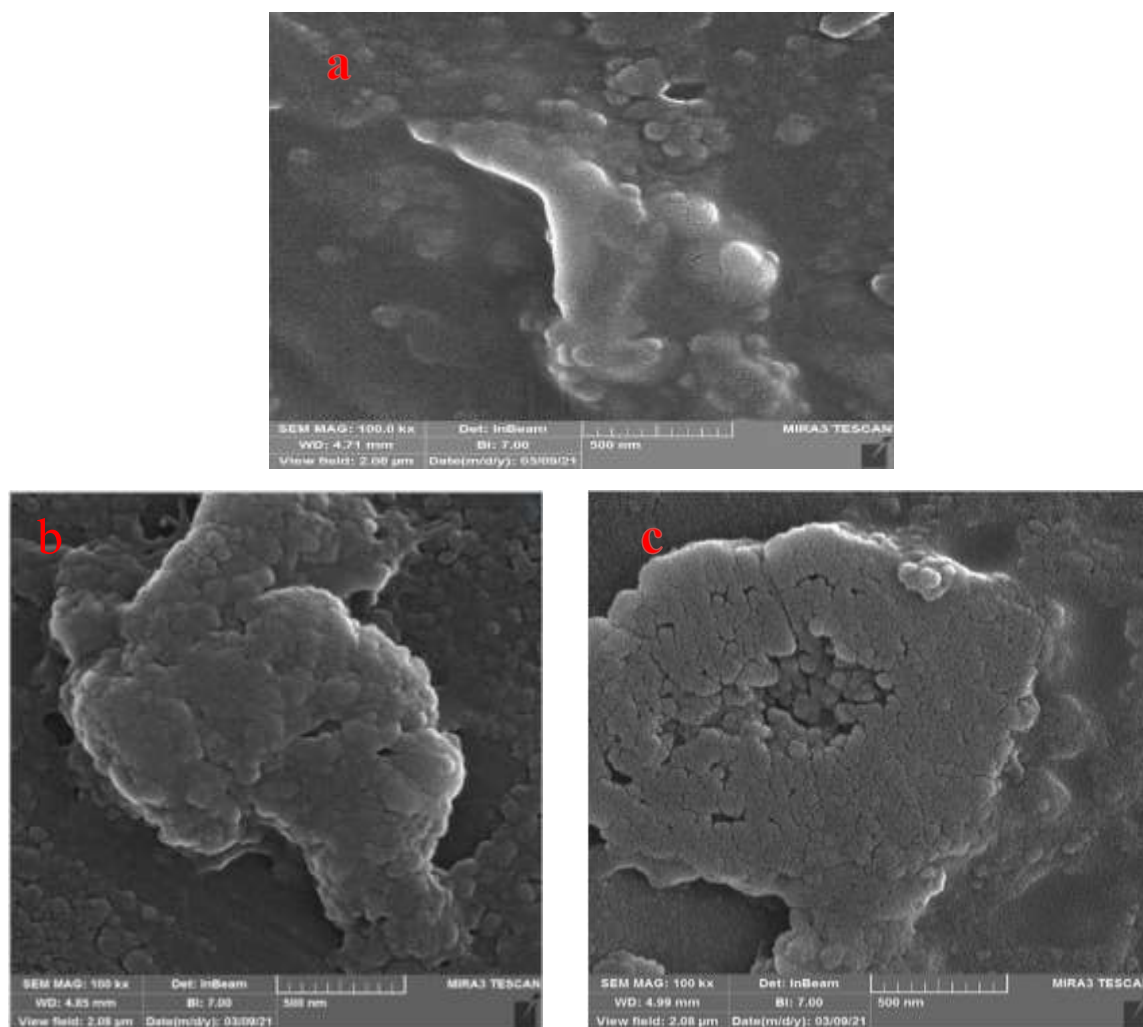


Figure 6: FE-SEM micrographs of TiO₂NPs synthesised with laser energy of (a) 80 mJ, (b) 120mJ, and (c) 160mJ at 100 pulses.

5. Conclusion

To summarize, we succeeded in preparing TiO₂ nanoparticles with characteristic crystal synthesis using a pulsed laser to ablate the submerged metal Ti target in deionized water (PLAL). Because of this technology, this method is simple, versatile, manageable, and less expensive. For the optical properties of NPs, the transmittance of the prepared TiO₂NPs decreased in the UV spectrum region and increased in the visible spectrum region with the increase in laser energy. The energy band gap for TiO₂NPs decreased from 3.89 to 3.7eV with the increase of laser energy from 80-160mJ, respectively. Also, the XRD analysis found the crystal structure of the as-prepared samples in a brookite phase. The nanoparticles have an identical cauliflower-like crystal shape, as shown in the SEM micrograph, and the amount of producing nanoparticles has increased with the increases in the laser energy.

Conflict of Interest:

Declaration by authors that there is no conflict of interest.

References

- [1] Boutinguiza, M., del Val, J., Riveiro, A., Lusquiños, *et al.*, "Synthesis of titanium oxide nanoparticles by ytterbium fiber laser ablation," *Physics Procedia*, vol. 41, p. 787-793, 2013.
- [2] Khashan, K S, Sulaiman, G M, Abdulameer, F A, *et al.*, "Antibacterial Activity of TiO₂ Nanoparticles Prepared by One-Step Laser Ablation in Liquid," *Applied Sciences*, vol. 11, p.4623, 2021
- [3] Ali, N., Taha, A., Ahmed, D.S., "Characterization of Treated Multi-Walled Carbon Nanotubes and Antibacterial Properties" *Journal of Applied Sciences and Nanotechnology*, vol.1, p.1-9, 2021,
- [4] Aboud, K.H., Imran, N.J., Al-Jawad, S.M.H., " Structural, Optical and Morphological Properties Cadmium Sulfide Thin Films Prepared by Hydrothermal Method" *Journal of Applied Sciences and Nanotechnology*, vol.1, p.49-57, 2021.
- [5] Solati, E., Aghazadeh, Z., & Dorrnian, D, "Effects of Liquid Ablation Environment on the Characteristics of TiO₂ Nanoparticles," *Journal of Cluster Science*, vol.31, p. 1-9, 2020.
- [6] Zhu, T. and Gao, S.P., "The stability, electronic structure, and optical property of TiO₂ polymorphs," *The Journal of Physical Chemistry C*, vol. 118(21), p.11385-11396, 2014.
- [7] Aziz, W. J., Ali, S. Q., & Jassim, N. Z., "Production TiO₂ Nanoparticles Using Laser Ablation in Ethanol," *Silicon*, vol.10(5), p.2101-2107,2018.
- [8] Singh, A., Vihinen, J., Frankberg, E., Hyvärinen, *et al.*, "Effect of laser power on yield of TiO₂ nanoparticles synthesized by pulsed laser ablation in water," *Journal of Ceramic Science and Technology*, vol.8, p.39-43, 2017.
- [9] Zuñiga-Ibarra, V. A., Shaji, S., Krishnan, B., Johny, *et al.*, "Synthesis and characterization of black TiO₂ nanoparticles by pulsed laser irradiation in liquid," *Applied Surface Science*, vol. 483, p.156-164, 2019.
- [10] N. Pashazadeh Kan, A. Najjigivi*, and A.H Sari, "Synthesis and Characterization of TiO₂ Nanoparticles by Pulsed Laser Ablation in Water: Effect of SDS incorporation," *International Journal of Nanotechnology in Medicine & Engineering*, vol.5:5, p.2474-8811, 2020.
- [11] Singh, A., Vihinen, J., Frankberg, E., Hyvärinen, L., Honkanen, M., & Levänen, E., "Pulsed Laser Ablation-Induced Green Synthesis of TiO₂ Nanoparticles and Application of Novel Small Angle X-Ray Scattering Technique for Nanoparticle Size and Size Distribution Analysis," *Nanoscale research letters*, vol.11(1),p. 1-9, 2016.
- [12] Sadrolhosseini, Amir Reza, *et al.*, "Laser ablated titanium oxide nanoparticles in carbon quantum dots solution for detection of sugar using fluorescence spectroscopy," *Materials Research Express*, 2021.
- [13] Mahdieh, M.H. and Fattahi, B., "Size properties of colloidal nanoparticles produced by nanosecond pulsed laser ablation and studying the effects of liquid medium and laser fluence," *Applied Surface Science*, vol.329, p.47-57, 2015.
- [14] R. K. Swarnkar, S. C. Singh and R. Gopal, "Effect of Aging on Copper Nanoparticles Synthesized by Pulsed Laser Ablation in Water: Structural and Optical Characterizations", *Bulletin of Materials Science*, Vol. 34, No. 7, p. 1363-1369,2011.
- [15] C. Sima, C. Viespe, C. Grigoriu, G. Prodan and V. Ciupina, "Production of Oxide Nanoparticles by Pulsed Laser Ablation," *Journal of Optoelectronics and Advanced Materials*, Vol. 10, No. 10, p. 2631 – 2636, 2008.
- [16] AL-Mosawi, B. T. S., "The use of laser ablation technique for the synthesis of titanium dioxide nanoparticles synergistic with sulfamethoxazole to prepare an anti-corrosion surface coating for mild steel and study of refraction and absorption," *International Journal of Corrosion and Scale Inhibition*, vol.9(3), p.1025-1036, 2020.
- [17] Thamir, A. D., Haider, A. J., & Ali, G. A., "Preparation of NanostructureTiO₂ at Different Temperatures by Pulsed Laser Deposition as Solar Cell," *Journal of Engineering Technology*, vol.34, p.193-204. 2016.
- [18] Khashan, K. S., "Synthesis, structure and optical properties of CdS nanoparticles prepared by chemical method," *Journal of Engineering Technology* 31, 39, 2013.
- [19] Andrade-Guel, M., Díaz-Jiménez, L., Cortés-Hernández, D. *et al.*, "Microwave assisted sol–gel synthesis of titanium dioxide using hydrochloric and acetic acid as catalysts," *Boletín de la Sociedad Española de Cerámica y Vidrio*, vol.58(4), p.171-177, 2019.
- [20] Al-Kinani, M.A., Haider, A.J. and Al-Musawi, S., "Study the Effect of Laser Wavelength on Polymeric Metallic Nanocarrier Synthesis for Curcumin Delivery in Prostate Cancer Therapy: In Vitro Study," *Journal of Applied Sciences and Nanotechnology*, Vol.1, No.1, p. 43-50 2021.
- [21] Khashan, K. S., Hadi, A., Mahdi, M., Hamid, M.K., "Nanosecond pulse laser preparation of InZnO (IZO)

- nanoparticles NPs for high-performance photodetector," *Applied Physics A*, vol.125, p.1-7. 2019
- [22] Ismail, R.A., Khashan, K. S., Alwan, A.M., "Study of the Effect of Incorporation of CdS Nanoparticles on the Porous Silicon Photodetector," *Silicon*, vol. 9, p.321, 2017.
- [23] Khashan,K.S., Abdulameer, F.A., Jabir, M.S., Hadi, A.A., Sulaiman G.M., "Anticancer activity and toxicity of carbon nanoparticles produced by pulsed laser ablation of graphite in water," *Advances in Natural Sciences: Nanoscience and Nanotechnology*,vol.11, p.035010, 2020.